Green Chemistry

PAPER

View Article Online
View Journal | View Issue

Cite this: *Green Chem.*, 2023, **25**, 6355

Carbonatation of [ethylene–glycidyl methacrylate]-based copolymers with carbon dioxide as a reagent: from batch to solvent-free reactive extrusion†

Bruno Guerdener, [a,b,c] Virgile Ayzac,[a] Sébastien Norsic,[a] Paul Besognet,[c] Véronique Bounor-Legaré,*[b] Vincent Monteil, *[a] Véronique Dufaud, *[a] Jean Raynaud *[a] and Yvan Chalamet*[c]

The carbonatation of semi-crystalline [ethylene–glycidyl methacrylate]-based polymers (Lotader® grades) was achieved using carbon dioxide as a reagent and quaternary ammonium salts as organo-catalysts to transform the polymers' epoxide pendant groups into cyclic carbonate moieties. A batch reactor allowed us to assess the kinetics, dependence on a catalyst and overall potential of this carbonatation. The influence of the ammonium salt composition (anion/cation) was studied in toluene at 110 °C to circumvent the high melting temperatures of these ethylene unit-rich copolymers and obtain a homogeneous medium. The amount of catalyst, CO_2 pressure and temperature were also optimized (TBAB, 5 mol% *vs.* epoxy content, 4.0 MPa, 110 °C) to allow for quantitative conversion of epoxides into cyclic carbonates. Subsequently, the reaction was transposed, for the 1st time, to reactive extrusion under CO_2 using a dedicated co-rotating twin-screw extruder to allow for CO_2 containment within the polymer melt. This solvent-free reactive process is perfectly adapted to semi-crystalline and/or high-T_g polymers. After optimization, a yield of up to 78% of cyclic carbonate, in addition to orthogonal epoxide, could be obtained with THAB (7.5 mol% *vs.* epoxy content, ~30 g h^{-1} of cat.) at 150 °C with an industry-compliant polymer flow rate of 2 kg h^{-1}. The respective reactivities of Lotader® grades were compared in batch and in an extruder, unveiling this trend towards carbonatation: AX8840 < AX8700 < AX8900. Sustainability and enhanced productivity of the carbonatation methodology developed herein relies on the use of CO_2 as a C1 reagent for the functionalization of epoxide-bearing polymers harnessing a continuous and clean reactive extrusion process allowing, in a single operation and a few minutes, the production of functional polymers at the kilogram scale under solvent-free conditions.

Received 6th April 2023,
Accepted 12th July 2023

DOI: 10.1039/d3gc01127e

rsc.li/greenchem

Introduction

The valorization of CO_2 into valuable chemical products has been extensively studied in recent years.[1–5] More specifically, the synthesis of carbonates *via* the reaction of mostly inert CO_2 with energy-rich epoxides has been the subject of great interest, due to the multiple industrial applications of cyclic carbonates[6–8] and the high atom efficiency of this transformation.[9]

Focusing on CO_2 upgrading for the advantageous derivatization of epoxides into cyclic carbonates (cycloaddition) or carbonate linkages (*e.g.* polymerization), one can indeed manufacture useful industrial platform molecules or benefit from the direct incorporation of CO_2 as a C1 building block in high-tonnage materials.[10–22] When post-modification of substrates more complex than simple epoxides is considered, *i.e.*, bio-sourced fatty acids,[23–28] bio-based epoxides[23,29–32] or synthetic

[a]*Univ. Lyon, Université Claude Bernard Lyon 1, CPE Lyon, CNRS, UMR 5128, Catalysis, Polymerization, Processes and Materials (CP2M), 43 Bd du 11 novembre 1918, 69616 Villeurbanne cedex, France. E-mail: vincent.monteil@univ-lyon1.fr, veronique.dufaud@univ-lyon1.fr, jean.raynaud@univ-lyon1.fr*
[b]*Univ. Lyon, CNRS, Université Claude Bernard Lyon 1, INSA Lyon, Université Jean Monnet, UMR 5223, Ingénierie des Matériaux Polymères, F-69622 Villeurbanne cedex, France. E-mail: veronique.bounor-legare@univ-lyon1.fr*
[c]*Univ. Lyon, CNRS, Université Claude Bernard Lyon 1, INSA Lyon, Université Jean Monnet, UMR 5223, Ingénierie des Matériaux Polymères, F-42023 Saint-Etienne cedex 2, France. E-mail: yvan.chalamet@univ-st-etienne.fr*

† Electronic supplementary information (ESI) available: Structure, properties and characterization of the commercial polymers, calibration curve for the quantitative determination of cyclic carbonates by IR-ATR, and characterization of the modified polymers with CO_2 in batch and in an extruder. See DOI: https://doi.org/10.1039/d3gc01127e

polymers featuring epoxide moieties,[33–40] this transformation may be relevant to improve the prospects of usability for (macro)molecules while utilizing abundant CO_2. There are two possible routes for the cycloaddition of CO_2 to epoxides depending on the nature of the chosen catalyst used. As catalysis is well reported and exemplified in the literature (see Schemes S1, S2 and the description of mechanisms in the ESI†),[41–67] it is very easy to select and tune the solubility/reactivity/selectivity of the catalyst system to the needs for specific carbonatation (physical properties, sterics and electronics of the substrates in particular).

Very interestingly, when CO_2 is used in post-polymerization as a derivatization agent (see Scheme 1), novel polymers bearing cyclic carbonate functional groups can be created. They have found applications in different sectors. They can be used as solid electrolytes thanks to their good lithium ion conductivity,[68] mixed with other polymers to create homogeneous films,[35] or can play the role of reactive compatibilizers.[69]

Moreover, cyclic carbonates and epoxides may show orthogonal reactivity: cyclic carbonates are more prone to react with amines than epoxides to produce, for example, hydroxyurethane functions,[11,14,15,20,68] and epoxides are more susceptible to hydrolysis than cyclic carbonates.[39]

However, in most cases, functionalization with CO_2 is carried out on polar polymers highly soluble in polar solvents in a batch reactor.[33–40] The chemical fixation of CO_2 to an apolar and semi-crystalline polymer bearing epoxide moieties is much more challenging (Scheme 1) because of the difficulties in obtaining an intimate and homogeneous mixture of the polymer, the CO_2 reactant and the catalyst.

In this work (see Scheme 1), we report on the development and optimization of the conditions for converting the epoxide groups of three different ethylene-containing copolymers, thus mostly apolar copolymers – Lotader® grades AX8900, AX8700 and AX8840 (see Scheme 2 and Scheme S3 in the ESI† for more details) – into the corresponding cyclic carbonates *via* the organocatalyzed cycloaddition of CO_2 (Scheme 3) in batch and by reactive extrusion processes. The reaction conditions were first investigated in batch for a better understanding of the influence of the different reaction parameters, and then transposed to a solvent-free reactive extrusion process in order to develop an original sustainable continuous process for the modification of epoxidized polymers with CO_2. This strategy allows for the introduction of a cyclic carbonate moiety in addition to and orthogonal to the remaining epoxides, which could prove valuable for a wide variety of material applications.[20,70,71]

We chose to pursue metal-free mediated CO_2 fixation methodologies for sustainability and material compatibility considerations and to avoid problematic metallic residues in the final polymer products. Among the organocatalysts developed so far to enable the efficient transformation of molecular epoxides, one can cite onium salts with ammonium or phosphonium halides, ionic liquids and organic bases. Their catalytic behavior towards glycidyl-methacrylate based polymers will be explored in the present work (Scheme 4).

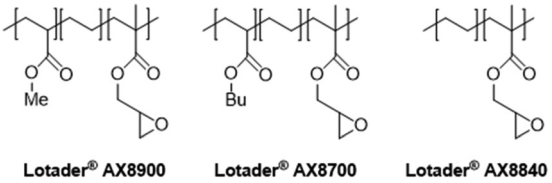

Scheme 2 Structure of Lotader® AX8900, AX8700 and AX8840.

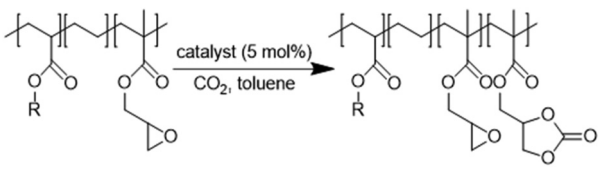

Scheme 3 Cycloaddition of CO_2 to Lotader®.

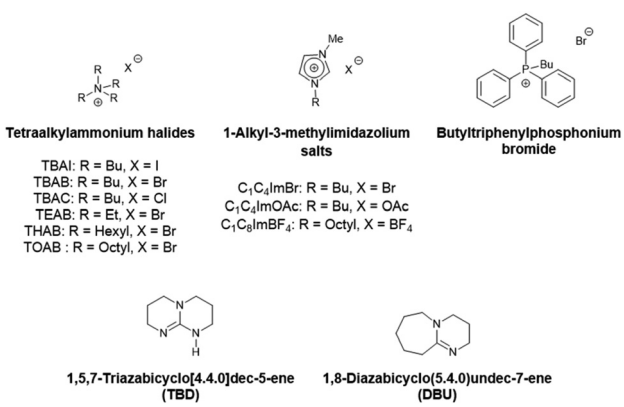

Scheme 4 Catalysts studied in this work.

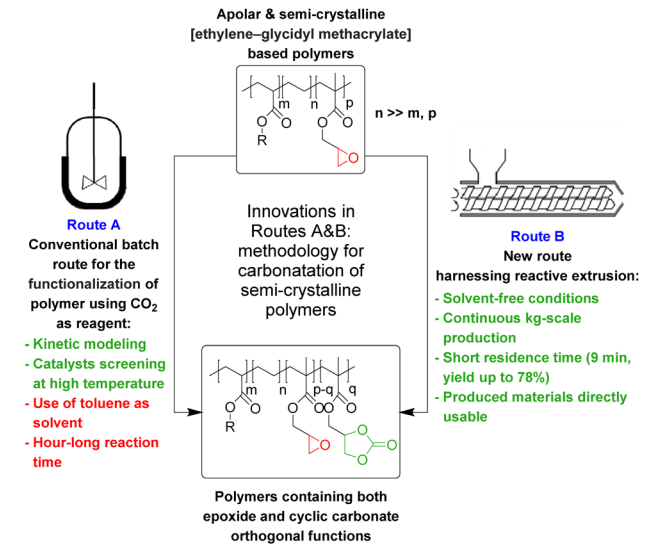

Scheme 1 Transposition of carbonatation from batch to reactive extrusion.

Results and discussion

Screening of the catalysts

First, commercially available organic salts such as tetrabutylammonium bromide (TBAB), butyltriphenylphosphonium bromide (PPh_3BuBr),1-butyl-3-methylimidazolium bromide (C_1C_4ImBr), 1-butyl-3-methylimidazolium acetate (C_1C_4ImOAc) and 1-methyl-3-octylimidazolium tetrafluoroborate ($C_1C_8ImBF_4$), and organic bases such as 1,5,7-triazabicyclo[4.4.0]dec-5-ene (TBD) and 1,8-diazabicyclo[5.4.0]undec-7-ene (DBU) were tested as catalysts for the cycloaddition of CO_2 to the Lotader® AX8900 under the following conditions: 110 °C, 5 h, 4.0 MPa of CO_2 and 5 mol% of catalyst. Toluene was used to solubilize the Lotader® AX8900. We did attempt to realize the transformation under "solvent-free" conditions in our batch reaction; however, very heterogeneous reaction media were obtained, even after 5 h of reaction (see Fig. S33 and Photo S1 of the ESI†), and inconsistent and low conversions in carbonates were achieved. Toluene is a good solvent for Lotader® grades and is easily accessible to most research teams. As shown in Table 1, epoxide activation with halide anions proved to be the best route to achieve satisfactory conversion (Table 1, entries 1–3), whereas only traces of cyclic carbonates were observed when using sterically hindered nucleophiles and bases (Table 1, entries 4–7). TBAB showed the best performance for the carbonatation of Lotader® AX8900 with a quantitative yield of cyclic carbonate (Table 1, entry 1). It should be noted that the imidazolium and phosphonium salts were only partially soluble in toluene at 110 °C unlike TBAB (completely soluble, even at room temperature), which may explain their low reactivity. The formation of the cyclic carbonate product was confirmed by IR-ATR (Fig. 1) and ^{1}H NMR (Fig. 2). After 5 hours of reaction of Lotader® AX8900 with CO_2 catalyzed by TBAB, the characteristic band of epoxide at 911 cm^{-1} disappeared with the concomitant appearance of the band at

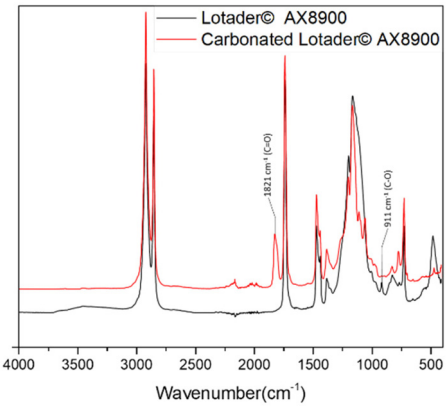

Fig. 1 IR-ATR spectra of the Lotader® AX8900 and the modified Lotader® AX8900 with CO_2 (Table 1, entry 1).

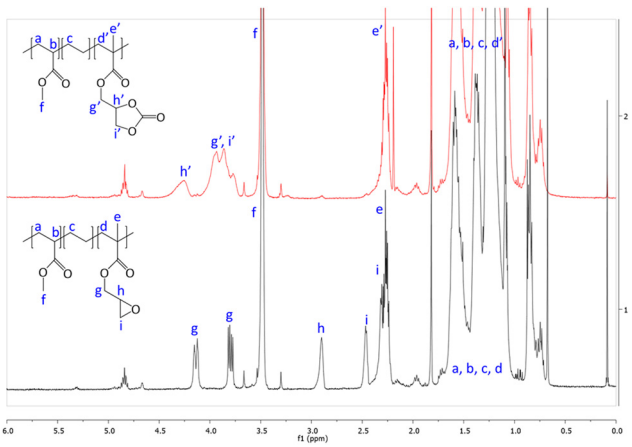

Fig. 2 ^{1}H NMR (TCE/C_6D_6, 400 MHz) spectra of Lotader® AX8900 and the modified Lotader® AX8900 with CO_2 (Table 1, entry 1) (see also Fig. S2 in the ESI† for further details).

Table 1 Screening of catalysts[a]

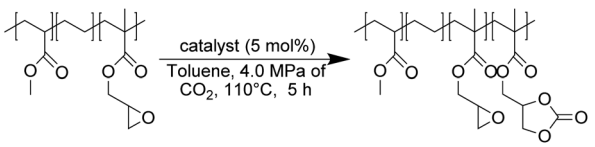

Entry	Catalyst	Yield[b] (%)
1	TBAB	99[c]
2	PPh_3BuBr	6
3	C_1C_4ImBr	24
4	$C_1C_8ImBF_4$	0
5	C_1C_4ImOAc	2
6	TBD	1
7	DBU	10

[a] Conditions: 2.0 g of Lotader® AX8900 (1.1 mmol of glycidyl methacrylate), 0.057 mmol of catalyst (5 mol%), 2.0 mL of toluene, 110 °C, 4.0 MPa of CO_2, 5 h. [b] Yield determined by IR-ATR using a calibration curve (see Fig. S18 in the ESI†). [c] Yield determined by ^{1}H NMR (see Fig. S20 in the ESI†).

1820 cm^{-1} typical of the C=O stretching vibration of cyclic carbonates[72] (Fig. 1). On the other hand, the ^{1}H NMR signals g, h and i related to the glycidyl methacrylate monomers almost disappeared and new signals h′, g′ and i′ corresponding to the carbonate product appeared.

Since tetrabutylammonium bromide proved to be the best performing catalyst, other key parameters such as the structural catalyst features and reaction conditions were assessed in the following studies using tetraalkylammonium halide salts with different substituents and counteranions.

Influence of the halide

The influence of the halide anion on the reaction kinetics is a crucial parameter to take into account as it is involved in epoxide ring-opening, the first step of the catalytic cycle. The pseudo-first order kinetics of the reaction was assessed with tetrabutylammonium iodide (TBAI) and TBAB (Fig. 3). Assuming that the concentrations of CO_2 and catalyst are con-

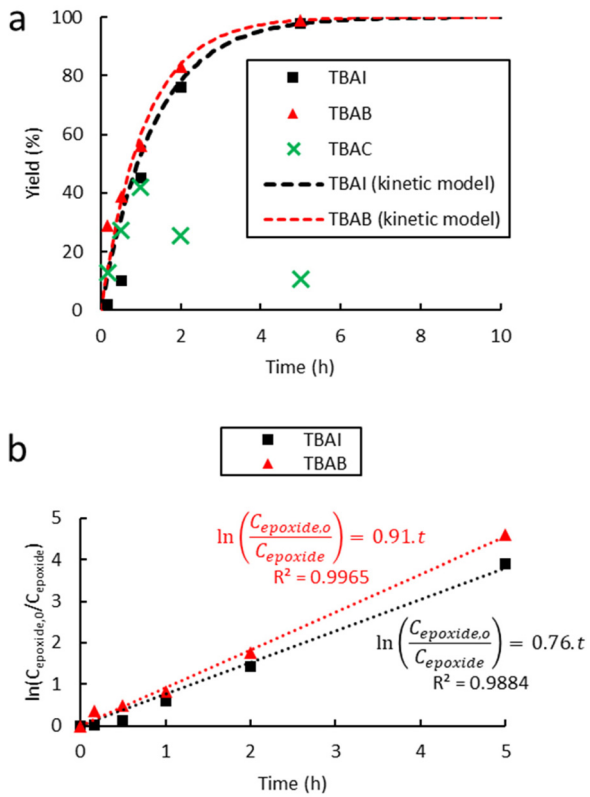

Fig. 3 Influence of the halide anion on the reaction kinetics in the cycloaddition of CO_2 to Lotader® AX8900: (a) plot of eqn (3) and (b) plot of eqn (2). Conditions: 2.0 g of Lotader® AX8900 (1.1 mmol of glycidyl methacrylate), 0.057 mmol of catalyst (5 mol%), 2.0 mL of toluene, 110 °C, 4.0 MPa of CO_2. Yield was determined by IR-ATR using a calibration curve (see Fig. S18 in the ESI†).

stant in the liquid phase over time, the reaction rate could be written as:

$$-\frac{dC_{epoxide}}{dt} = k_{obs} \cdot C^{a}_{epoxide} \quad (1)$$

where $k_{obs} = k \cdot C^{b}_{CO_2} \cdot C^{c}_{catalyst}$.

If the reaction follows the pseudo-first order kinetics, the differential equations can be integrated, and k_{obs} can be estimated as:

$$\ln\left(\frac{C_{epoxide,o}}{C_{epoxide}}\right) = k_{obs} \cdot t \quad (2)$$

As no side-reaction was observed with TBAI and TBAB, the yield of the cyclic carbonate product is equal to the conversion of the epoxide moiety and can be expressed as follows:

$$\text{Yield} = 1 - e^{-k_{obs} \cdot t}. \quad (3)$$

Fig. 3 shows the plots of eqn (2) and (3). From these data the rate constant k_{obs} was estimated to be 0.76 h^{-1} and 0.91 h^{-1} for the reaction catalyzed with respectively TBAI and TBAB, suggesting that Br^- has a higher catalytic activity than I^-. In the case of the carbonatation of terminal molecular epoxides under neat conditions or in apolar solvents such as toluene, the order of activity follows the order of halide nucleophilicity and leaving group ability: I^- > Br^- > Cl^- > F^-.[41,45,53,64,65,73–75] But in the case of the carbonatation of sterically hindered terminal epoxides, a good balance between the halide size and its leaving group ability is required.[72,75] A too voluminous and polarizable halide would not favor the attack of the halide on the epoxide, which could explain why I^- is less active than Br^-.

In the case of tetrabutylammonium chloride (TBAC), the consumption of the formed cyclic carbonates was observed after 1 h of reaction at 110 °C (Fig. 3(a)), which could be due to a secondary reaction, leading to a polymer less or even non-soluble in toluene, likely due to crosslinking, compared to the modified polymers obtained with TBAI and TBAB. Ochiai *et al.* observed a similar behaviour with CO_2 fixation to poly(glycidyl methacrylate-*co*-methyl methacrylate) catalyzed by tetrabutylammonium fluoride (TBAF) and suggested that polymerization of the sole epoxide to polyethers was favored due to the weak leaving group ability of the fluoride anion.[36] Once enough cyclic carbonate species are generated, a direct nucleophilic attack of the alkoxide on the carbonate ring with subsequent decarboxylation could yield several polyether repeating units leading to some insoluble material, which was also observed in our case (see Scheme 5 and the CPMAS-NMR spectra of Fig. S24 in the ESI†).

Influence of the alkyl chains

Ammonium bromide salts such as tetraethylammonium bromide (TEAB), TBAB, tetrahexylammonium bromide (THAB) and tetraoctylammonium bromide (TOAB) were chosen to study the influence of the alkyl chains' length. As shown in Fig. 4, one can observe that the length does influence the catalytic activity. After 1 h of reaction at 110 °C, the following catalytic reactivity order was obtained: TEAB ≪ TOAB ≈ TBAB < THAB. These results showed that increasing the length of the alkyl chains, while improving solubility in the apolar medium, makes the ammonium cation bulkier and thus decreases the electrostatic interactions between the ion pairs. This results in greater nucleophilicity of the anion and hence enhanced reactivity.[45] While the larger ammonium cation showed satisfac-

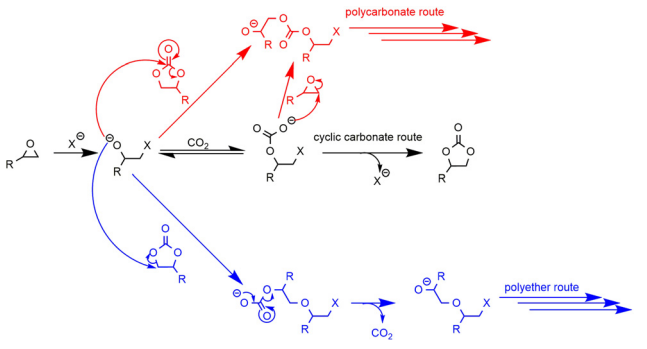

Scheme 5 Potential side-reaction of epoxide with CO_2. [See also ref. 36].

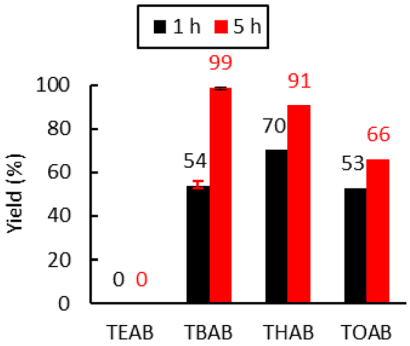

Fig. 4 Influence of the alkyl chains on the tetraalkylammonium bromide activity. Conditions: 2.0 g of Lotader® AX8900 (1.1 mmol of glycidyl methacrylate), 0.057 mmol of catalyst (5 mol%), 2.0 mL of toluene, 110 °C, 4.0 MPa of CO_2. Yield determined by IR-ATR using a calibration curve (see Fig. S18 in the ESI†).

tory activity at a short reaction time (more than 50% yield after 1 hour), TEAB was completely inactive due to its insolubility in toluene. It has also been shown that a too bulky cation should disfavor the formation of the alkoxide intermediate,[72] explaining why TOAB was less active than THAB.

However, after 5 h at 110 °C, the catalytic reactivity order changed as follows: TEAB ≪ TOAB < THAB < TBAB. This could be explained by the fact that the bulkier the ammonium, the less stabilized the alkoxide intermediate, because of the decrease of the electrostatic interactions between the ion pairs. It would favor parallel side reactions between the alkoxides and the cyclic carbonates to produce polyether units *via* decarboxylation reactions, as reported before (see Scheme 5 and the CPMAS-NMR spectra of Fig. S24†).[36] The overall enhanced solubility of the cation and ion pair dissociation could thus be a determining factor for improved kinetics at early stages, but a trade-off in terms of cation size would be ideal when it comes to selectivity over longer reaction times (see Fig. 4).

Influence of the reaction parameters

The dependence of the cyclic carbonate yield on the CO_2 pressure was investigated at 110 °C for a period of 1 h using TBAI as a catalyst. As shown in Fig. 5(a), increasing the pressure from 2 to 4 MPa led to an increase of the yield from 15% to 45%. This could be due to a higher concentration of CO_2 in the liquid phase, which may both increase the kinetic rate and reduce the viscosity of the reaction mixture *via* plasticization of the polymer, as already reported for other polymers.[76,77] Beyond 4 MPa, the yield reaches a plateau and starts to slightly decrease from 10 MPa. This decrease in the yield with an increase of CO_2 pressure has previously been observed in the case of molecular epoxides,[43,45] with the supercritical state of CO_2 affecting the solubility of each component in the continuous phase through dilution or even forcing precipitation in our case.[78] Thus, a pressure of 4 MPa seems ideal for TBAI to operate efficiently. The influence of the amount of TBAI on catalytic performance was also studied (4.0 MPa of CO_2, 110 °C, 1 h). The results in Fig. 5(b) show that increasing

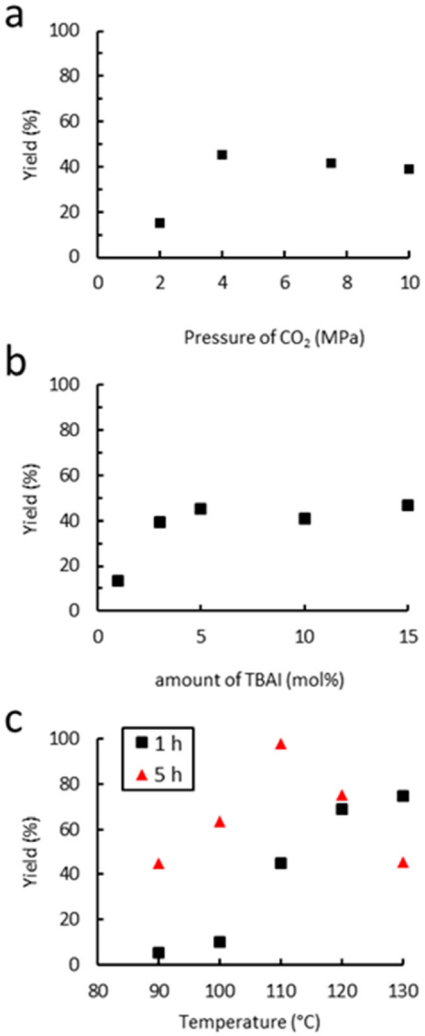

Fig. 5 Influence of (a) the CO_2 pressure, (b) amount of TBAI and (c) temperature on catalytic performance. Unless otherwise mentioned, reaction conditions: 2.0 g of Lotader® AX8900 (1.1 mmol of glycidyl methacrylate), 0.057 mmol of TBAI (5 mol%), 4.0 MPa of CO_2, 2.0 mL of toluene, 110 °C, 1 h. Yield determined by IR-ATR using a calibration curve (see Fig. S18 in the ESI†).

the concentration of TBAI from 1 to 5 mol% led to a marked improvement of the yield from 13 to 45%. A further increase of the quantity of TBAI up to 15 mol% did not lead to further activity improvement. Thus, the TBAI catalyst concentration was set at 5 mol%.

Finally, the influence of the temperature on the carbonatation reaction of Lotader® AX8900 was studied (4.0 MPa of CO_2, 5 mol% TBAI) as it could greatly impact both the reaction rate and the solubility/viscosity of the reaction medium particularly when polymers are at stake. The results shown in Fig. 5(c) reveal that the reaction temperature strongly affects catalyst reactivity as very low yields were obtained after 1 hour of reaction below 100 °C. Increasing the temperature further from 100 to 120 °C led to a significant improvement in the yield of the cyclic carbonate product from 5 to 65%. A further increase of the temperature up to 130 °C did not lead to significant

activity improvement. As stated above, the temperature may influence the kinetic rate and improve the gas–liquid transfer but partial or total degradation of the catalyst may also occur with the temperature increase. However, after 5 hours, an increase of the temperature from 110 °C to 130 °C led to a decrease of the yield from 99% to 45%. It could be explained by the formation of polyether repeating units and thus the consumption of the cyclic carbonate moiety *via* decarboxylation, as reported previously.[36] Therefore, the influence of the acrylate comonomer in the polymer structure on the reaction efficiency was assessed under the following optimal conditions: TBAB (5 mol%), 4 MPa of CO_2, 110 °C, 5 h.

Influence of the acrylate comonomer

The Lotader® AX8900, AX8700 and AX8840 were functionalized with CO_2 under optimal conditions to study the influence of the acrylate comonomer (type or presence) on the reaction efficiency. It is notable that the three polymers are soluble in toluene at 110 °C at a concentration of 1 g of polymer per mL of toluene.

Under these conditions, the factors that could influence the reaction outcome are the polarity of the polymer, the molar mass of the Lotader®, the CO_2 solubility in the liquid phase and the viscosity of the liquid phase. The results presented in Table 2 show that the reactivity of the polymer increases in the following order: AX8840 < AX8700 < AX8900, which also mirrors the polarity order. AX8700 is more apolar than AX8900 because of the presence of butyl groups instead of methyl groups, and AX8840 is even more apolar because of the absence of the acrylate comonomer. This change of polarity may affect the CO_2 solubility in the liquid phase. It is well known that CO_2 is more soluble in relative polar media, due to its significant quadrupole moment.[79] The ester groups of the acrylate comonomer may interact with CO_2 and favor its solubility, thus favoring the reaction with the epoxide moieties.

Methodology transposition to reactive extrusion

The aforementioned autoclave results showed that ammonium halides were the most active catalysts for the carbonatation of Lotader® in toluene solution. Specifically, the use of TBAB, THAB and TBAI as catalysts provided the highest yields of cyclic carbonates, up to 99% after 5 hours of reaction at 110 °C in the case of TBAB. These catalysts were therefore chosen for the carbonatation of Lotader® by reactive extrusion. Due to its flexibility in screw design and easily adjustable temperature profiles, the extrusion process has remarkable mixing and homogenization capabilities for viscous systems in the molten state. Thus, the use of an extruder as a continuous reactor makes it possible to avoid resorting to hazardous solvents, which are always difficult to extract industrially (costly devolatilization step). The reactive extrusion process is thus often considered as a promising green process, allowing for the continuous production of large quantities of modified polymers.

The use of CO_2 [79] as a reagent for the carbonatation of polymers by a reactive extrusion process[80,81] has never been reported before. In contrast to radical processes, catalytic processes within reactive extruders are also extremely rare to the best of our knowledge, in particular in the realm of polymer functionalization.[82,83]

This constitutes a significant step forward since it both offers a solvent-free alternative and a scalable process amenable to industrial eco-design requirements. The transposition of the batch process to reactive extrusion was possible thanks to the adjustments of the batch reaction conditions. A co-rotating twin-screw extruder fed with the Lotader®, the catalyst and CO_2 was used to perform the experiments, at a flow rate of 2 kg h^{-1} and a rotational speed of 150 rpm. The overall design of this process is depicted in Scheme S4 (ESI†): it provides containment of CO_2 pressure within the polymer melt for carbonatation to proceed (see also Photo S2 in the ESI†).

The minimal temperature for the extrusion of the different Lotader® was determined experimentally to be 120 °C (over the melting points of the Lotader® AX8900, AX8700 and AX8840, which are respectively 65 °C, 72 °C and 104 °C).

Furthermore, the different twin-screw extruder parameters had to be optimized to obtain good yields, as a very short average residence time of 9 minutes has been precisely determined *via* colorimetric measurements, compared to the hour-long reaction times in the batch process.

First, the influence of extrusion temperature and CO_2 pressure was studied on the carbonatation of Lotader® AX8900 (Scheme 6). As shown in Fig. 6(a), an increase in temperature led to an increase in carbonate yield. The optimum pressure was 4.0 MPa, which is probably a good compromise between maximal CO_2 solubilization/availability for reaction and the avoidance of phase separation in the melt. At this pressure, an increase of 10 °C led to an average yield increase of 15%.

Table 2 Influence of the alkyl acrylate monomer

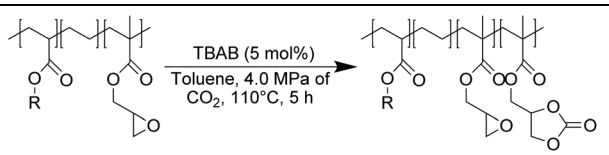

Entry	R	Polymer	Yield (%)
1	Me	Lotader® AX8900	99
2	Bu	Lotader® AX8700	82
3	—	Lotader® AX8840	62

Reaction conditions: 2.0 g of polymer (1.1 mmol of glycidyl methacrylate), 18 mg of TBAB (0.057 mmol, 5 mol%), 4.0 MPa of CO_2, 2.0 mL of toluene, 110 °C, 5 h. Yield determined by ^{1}H NMR (see Fig. S20, S21 and S22 in the ESI†).

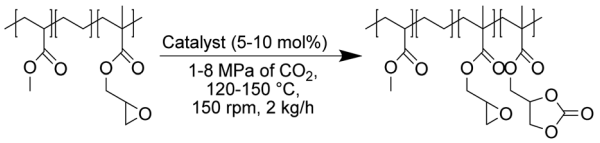

Scheme 6 Carbonatation of Lotader® AX8900 in an extruder.

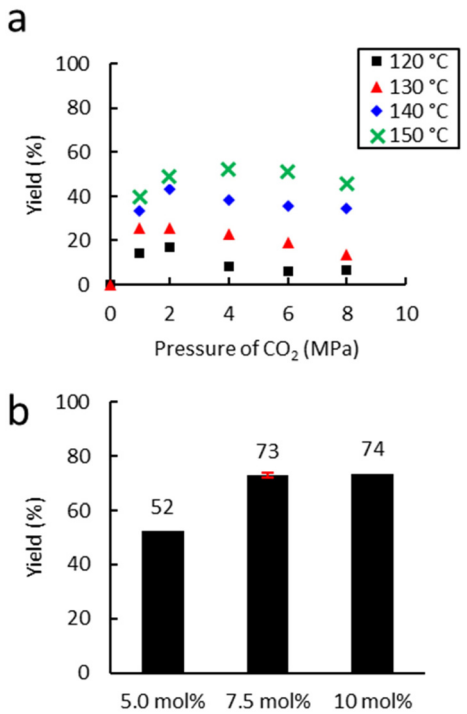

Fig. 6 Influence of (a) temperature and (b) the amount of catalyst. Unless otherwise mentioned, reaction conditions: 2 kg h^{-1} of Lotader® AX8900, 18 g h^{-1} of TBAB (5 mol%), 150 °C, 150 rpm. Yield determined by IR-ATR using a calibration curve (see Fig. S18 ESI†).

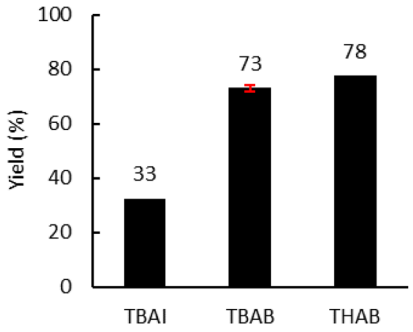

Fig. 7 Influence of the nature of the catalyst. Unless otherwise mentioned, reaction conditions: 2 kg h^{-1} of Lotader® AX8900, 0.086 mol h^{-1} of catalyst (7.5 mol%), 150 °C, 4 MPa of CO_2, 150 rpm. Yield determined by IR-ATR using a calibration curve (see Fig. S18 in the ESI†).

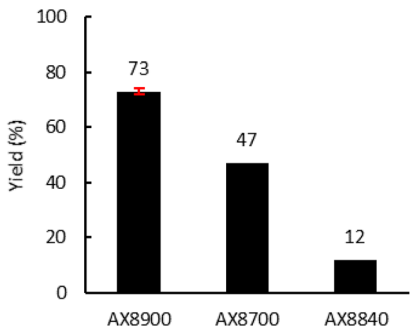

Fig. 8 Influence of the acrylate monomer. Reaction conditions: 2 kg h^{-1} of Lotader®, 0.086 mol h^{-1} of TBAB (7.5 mol%, 27 g h^{-1} of cat.), 150 °C, 4 MPa of CO_2, 150 rpm. Yield determined by ^{1}H NMR (see Fig. S44, S45 and S46 in the ESI†).

The temperature was not increased above 150 °C to avoid catalyst degradation that starts from 160 °C according to TGA analyses (see Fig. S61 and S62 in the ESI†).

Moreover, the amount of catalyst was optimized (Fig. 6(b)) with 4.0 MPa of CO_2. An increase from 5.0 to 7.5 mol% led to a significant increase in yield from 53% to 72%. A further increase to 10 mol% did not lead to a significant improvement in the yield. Subsequently, the influence of the nature of the catalyst was investigated under optimal conditions (7.5 mol% catalyst, 150 °C, 150 rpm, 2 kg h^{-1}) (Fig. 7). With TBAI, a low yield of 33% was obtained. This could be explained by the fact that the melting temperature of TBAI is 155 °C, thus it is in solid form during extrusion. The catalyst would therefore be less homogeneously dispersed within the polymer matrix, which would reduce the cyclic carbonate yield. Regarding TBAB and THAB, a similar activity to that in the batch reactor was obtained, with a yield of 72% and 78% respectively. With their melting point being at about 100 °C, their liquid state under the reaction conditions may improve their dispersion in the medium and not affect their activity.

Finally, the Lotader® AX8700 and AX8840 were also modified with CO_2 in reactive extrusion under optimal conditions (TBAB (7.5 mol%), 150 °C, 150 rpm, 2 kg h^{-1}) (Fig. 8). The same reactivity order as that obtained in batch was observed: AX8840 ≪ AX8700 < AX8840. Interestingly, as previously observed for the batch process, the integrity of the polymer chains is retained throughout the process, and even more so using the reactive extrusion process (high T °C but a low residence time *vs.* long shear stress stirring) as evidenced by the polymer characteristics displayed in Table S2 (ESI†).

Conclusions

Ethylene–glycidyl methacrylate based copolymers were successfully functionalized with carbon dioxide using commercial and non-toxic tetraalkylammonium halide catalysts, leading to the formation of cyclic carbonate pendant groups on the polymer chain, in a batch reactor and an extruder. The influences of the catalyst structure and the reaction parameters were evaluated in batch and it was found that TBAI, THAB and TBAB were the most active catalysts, with TBAB achieving up to 99% yield of cyclic carbonate.

The difference in reactivity between Lotader® AX8900, AX8700 and AX8840 suggested that the presence of polar groups, such as esters derived from acrylate comonomers, in the polymer structure may increase the CO_2 solubility and facilitate its approach to the epoxide moieties.

The procedure developed in an autoclave has been successfully transposed to a solvent-free reactive extrusion process,

with a yield of cyclic carbonate up to 78% using THAB as the catalyst on the Lotader® AX8900, allowing access to cyclic carbonates in addition to the remaining epoxides. Modifications of AX8700 and AX8840 were also successful. These modified [cyclic carbonate + epoxide]-featuring polymers may have several direct applications *e.g.* as intermediates for the synthesis of polyhydroxyurethanes, as reactive compatibilizers for blends of polyolefins with polyamides, polyesters, polyacids and polycarbonates, and could also display good permeability properties for membranes. The enhanced sustainability of our reactive extrusion process (kg-scale production of functionalized polymers in a continuous fashion under solvent-free conditions using CO_2 as a direct C1 source) could pave the way for other industrially-relevant (co)polymers.

Experimental part

Materials and equipment

Lotader® AX8900, AX8840 and AX8700 were purchased from Arkema. CO_2 was purchased from Air Liquide and the purity was 99.995%. For the batch study, 1-butyl-3-methylimidazolium acetate was purchased from Strem Chemicals. Toluene and all the other catalysts were supplied by Sigma Aldrich. For the reactive extrusion optimization, TBAB and TBAI were purchased from TCI Chemicals and THAB was purchased from Sigma Aldrich. All the chemicals were used without further purification.

All batch reactions were performed in a 0.16 L stainless steel reactor.

The reactive extrusion experiments were conducted in a twin-screw extruder, a BC 21 (L/D = 36, screw diameter = 25 mm) from Clextral, using a co-rotative configuration. The extruder had 9 barrels, numbered consecutively from 1 to 9 from the feed port to the die. The die had a diameter of 3 mm and a length of 10 mm. The extruder had 9 heating zones.

Analytical methods

^{1}H NMR spectra were recorded using a Bruker 400 Avance III, and ^{13}C NMR spectra were recorded using a Bruker Avance II. A TCE/C_6D_6 (2/1) (v/v) mixture was used as a deuterated solvent. All NMR analyses were performed at 363 K. All chemical shifts were measured relative to residual ^{1}H or ^{13}C resonance in the deuterated solvent: 7.16 ppm for ^{1}H and 128.06 ppm for ^{13}C.

IR-ATR measurements were performed at room temperature on Nicolet i550 FT-IR apparatus on the native and modified polymers. Characteristic bonds are cyclic carbonate C=O (1820–1822 cm^{-1}), ester C=O (1734 cm^{-1}) and epoxide C–O (911 cm^{-1}).

General procedures (typical carbonatation processes; more details in the ESI†)

Typical procedure for the functionalization of Lotader® AX8900 with CO_2 in the batch reactor. 2.0 g of Lotader® AX8900 (1.1 mmol of glycidyl methacrylate), 18 mg of TBAB (0.056 mmol, 5 mol%) and 2.0 mL of toluene were added in a 0.16 L stainless steel reactor. The reactor was sealed, and then the mixture was stirred at 300 rpm and heated up to 110 °C. When the desired temperature was reached, 4.0 MPa of CO_2 was introduced. The mixture was stirred at 300 rpm and 110 °C for 5 hours. Finally, CO_2 was degassed, the medium was dried under vacuum and the resultant polymer was recovered without further purification. A cyclic carbonate moiety was obtained with a yield of 99% according to ^{1}H NMR.

Typical procedure for the functionalization of Lotader® AX8900 with CO_2 in the reactive extruder. The Lotader® AX8900 and the catalyst were fed at a throughput of 2 kg h^{-1} (1.1 mol h^{-1} of glycidyl methacrylate) and 0.083 mol h^{-1} (7.5 mol%) respectively in the first barrel. Under optimal conditions, the temperatures were 60, 120, 150, 150, 150, 150, 150, 150 and 150 °C, respectively. The die was also heated to 150 °C. The screw speed was 150 rpm. When the flow of the extruded polymer was stabilized, CO_2 was continuously injected into the third barrel using a Linde pump (DSD 500). The pressure and the throughput were regulated by the pump. The resulting modified Lotader® AX8900 had a stable composition after a time equal to twice the residence time, and thus it was collected from this moment, cooled with compressed air and pelletized by a pelletizer.

Excellent reproducibility was observed for both techniques, providing conversions within the 2–3% range of deviation between repeated experiments. This is likely due to excellent mixing both for the toluene-assisted batch process (see in particular Fig. S19, ESI†) and for the reactive extrusion (intimate mixing of the polymer melt under CO_2 pressure), providing homogenised reaction media (see Fig. 6, 7 & 8 for TBAB as a catalyst: small error bars).

Typical procedure for the determination of the residence time by colorimetry in the reactive extruder. The first barrel of the extruder received the Lotader® AX8900 at a throughput of 2 kg h^{-1}, the temperatures of the 9 barrels were 60, 120, 150, 150, 150, 150, 150, 150 and 150 °C, respectively. The die was also heated to 150 °C. The screw speed was 150 rpm. When the flow of the extruded polymer was stabilized, 0.5 g of a magenta pigment was introduced into the first barrel, and the evolution of the extruded polymer colour was followed by colorimetry.

Author contributions

All of the experiments were conducted by B. G. and V. A., and processes were supervised by S. N. and P. B. All the authors contributed to the preparation of this manuscript. Conceptualization: V. B.-L., V. D., Y. C., V. M. and J. R.; writing-original draft, review, and editing: B. G., V. B.-L., V. D., Y. C., V. M. and J. R.

Conflicts of interest

The authors are also the inventors of a French patent application deposited under the number FR2300220 and not yet published.

Acknowledgements

The authors would like to thank the Institut Carnot Ingénierie@Lyon for financial support, with in particular the PhD fellowship of BG and post-doctoral contract of VA, Axel'One Campus for the NMR analyses and "La plateforme lyonnaise de caractérisation des Polymères" for the SEC analyses.

References

1 T. Sakakura, J.-C. Choi and H. Yasuda, *Chem. Rev.*, 2007, **107**, 2365–2387.
2 M. Aresta, A. Dibenedetto and A. Angelini, *Chem. Rev.*, 2014, **114**, 1709–1742.
3 Q. Liu, L. Wu, R. Jackstell and M. Beller, *Nat. Commun.*, 2015, **6**, 5933.
4 X. Lim, *Nature*, 2015, **526**, 628–630.
5 C. Hepburn, E. Adlen, J. Beddington, E. A. Carter, S. Fuss, N. Mac Dowell, J. C. Minx, P. Smith and C. K. Williams, *Nature*, 2019, **575**, 87–97.
6 A.-A. G. Shaikh and S. Sivaram, *Chem. Rev.*, 1996, **96**, 951–976.
7 J. H. Clements, *Ind. Eng. Chem. Res.*, 2003, **42**, 663–674.
8 B. Schäffner, F. Schäffner, S. P. Verevkin and A. Börner, *Chem. Rev.*, 2010, **110**, 4554–4581.
9 Y. Du, F. Cai, D.-L. Kong and L.-N. He, *Green Chem.*, 2005, **7**, 518.
10 D. J. Darensbourg, *Chem. Rev.*, 2007, **107**, 2388–2410.
11 A. Boyer, E. Cloutet, T. Tassaing, B. Gadenne, C. Alfos and H. Cramail, *Green Chem.*, 2010, **12**, 2205.
12 M. R. Kember, A. Buchard and C. K. Williams, *Chem. Commun.*, 2011, **47**, 141–163.
13 C. Romain and C. K. Williams, *Angew. Chem., Int. Ed.*, 2014, **53**, 1607–1610.
14 L. Maisonneuve, A.-L. Wirotius, C. Alfos, E. Grau and H. Cramail, *Polym. Chem.*, 2014, **5**, 6142–6147.
15 L. Maisonneuve, O. Lamarzelle, E. Rix, E. Grau and H. Cramail, *Chem. Rev.*, 2015, **115**, 12407–12439.
16 Y. Zhu, C. Romain and C. K. Williams, *Nature*, 2016, **540**, 354–362.
17 N. Kindermann, À. Cristòfol and A. W. Kleij, *ACS Catal.*, 2017, **7**, 3860–3863.
18 B. Grignard, S. Gennen, C. Jérôme, A. W. Kleij and C. Detrembleur, *Chem. Soc. Rev.*, 2019, **48**, 4466–4514.
19 A. C. Deacy, E. Moreby, A. Phanopoulos and C. K. Williams, *J. Am. Chem. Soc.*, 2020, **142**, 19150–19160.
20 S.-E. Dechent, A. W. Kleij and G. A. Luinstra, *Green Chem.*, 2020, **22**, 969–978.
21 A. C. Deacy, G. L. Gregory, G. S. Sulley, T. T. D. Chen and C. K. Williams, *J. Am. Chem. Soc.*, 2021, **143**, 10021–10040.
22 X. Liu, X. Yang, S. Wang, S. Wang, Z. Wang, S. Liu, X. Xu, H. Liu and Z. Song, *ACS Sustainable Chem. Eng.*, 2021, **9**, 4175–4184.
23 L. Longwitz, J. Steinbauer, A. Spannenberg and T. Werner, *ACS Catal.*, 2018, **8**, 665–672.
24 N. Tenhumberg, H. Büttner, B. Schäffner, D. Kruse, M. Blumenstein and T. Werner, *Green Chem.*, 2016, **18**, 3775–3788.
25 F. Chen, Q.-C. Zhang, D. Wei, Q. Bu, B. Dai and N. Liu, *J. Org. Chem.*, 2019, **84**, 11407–11416.
26 W. Liu, G. Lu, B. Xiao and C. Xie, *RSC Adv.*, 2018, **8**, 30860–30867.
27 A. Akhdar, K. Onida, N. D. Vu, K. Grollier, S. Norsic, C. Boisson, F. D'Agosto and N. Duguet, *Adv. Sustainable Syst.*, 2021, **5**, 2000218.
28 J. Catalá, M. P. Caballero, F. de la Cruz-Martínez, J. Tejeda, J. A. Castro-Osma, A. Lara-Sánchez, J. M. García-Vargas, M. T. García, M. J. Ramos, I. Gracia and J. F. Rodríguez, *J. CO2 Util.*, 2022, **61**, 102060.
29 H. Morikawa, M. Minamoto, Y. Gorou, J. Yamaguchi, H. Morinaga and S. Motokucho, *Bull. Chem. Soc. Jpn.*, 2018, **91**, 92–94.
30 A. Rehman, A. M. López Fernández, M. F. M. Gunam Resul and A. Harvey, *J. CO2 Util.*, 2019, **29**, 126–133.
31 F. de la Cruz-Martínez, M. Martínez de Sarasa Buchaca, J. Martínez, J. Fernández-Baeza, L. F. Sánchez-Barba, A. Rodríguez-Diéguez, J. A. Castro-Osma and A. Lara-Sánchez, *ACS Sustainable Chem. Eng.*, 2019, **7**, 20126–20138.
32 M. Navarro, L. F. Sánchez-Barba, A. Garcés, J. Fernández-Baeza, I. Fernández, A. Lara-Sánchez and A. M. Rodríguez, *Catal. Sci. Technol.*, 2020, **10**, 3265–3278.
33 N. Kihara and T. Endo, *Macromolecules*, 1992, **25**, 4824–4825.
34 J.-Y. Moon, H.-J. Jang, K.-H. Kim, S.-E. Na, D.-W. Park and J.-K. Lee, *Korean J. Chem. Eng.*, 1999, **16**, 721–724.
35 S. Y. Park, H. Y. Park, D. W. Park and C. S. Ha, *J. Macromol. Sci., Part A: Pure Appl.Chem.*, 2002, **39**, 573–589.
36 B. Ochiai, T. Iwamoto, K. Miyazaki and T. Endo, *Macromolecules*, 2005, **38**, 9939–9943.
37 S. Park, B. Choi, B. Lee, D. Park and S. Kim, *Sep. Sci. Technol.*, 2006, **41**, 829–839.
38 B. Ochiai, Y. Hatano and T. Endo, *J. Polym. Sci., Part A: Polym. Chem.*, 2009, **47**, 3170–3176.
39 B. Ochiai and T. Nakayama, *J. Polym. Sci., Part A: Polym. Chem.*, 2010, **48**, 5382–5390.
40 B. Liu, Y.-Y. Zhang, X.-H. Zhang, B.-Y. Du and Z.-Q. Fan, *Polym. Chem.*, 2016, **7**, 3731–3739.
41 V. Caló, A. Nacci, A. Monopoli and A. Fanizzi, *Org. Lett.*, 2002, **4**, 2561–2563.
42 H. Kim, *J. Catal.*, 2003, **220**, 44–46.
43 H. Kawanami, A. Sasaki, K. Matsui and Y. Ikushima, *Chem. Commun.*, 2003, 896–897.
44 D. J. Darensbourg, S. J. Lewis, J. L. Rodgers and J. C. Yarbrough, *Inorg. Chem.*, 2003, **42**, 581–589.
45 J. Sun, S.-I. Fujita, F. Zhao and M. Arai, *Appl. Catal., A*, 2005, **287**, 221–226.
46 H. Sugimoto and K. Kuroda, *Macromolecules*, 2008, **41**, 312–317.
47 A. Sibaouih, P. Ryan, M. Leskelä, B. Rieger and T. Repo, *Appl. Catal., A*, 2009, **365**, 194–198.

48 T. Seki, J.-D. Grunwaldt and A. Baiker, *J. Phys. Chem. B*, 2009, **113**, 114–122.
49 T. Chang, L. Jin and H. Jing, *ChemCatChem*, 2009, **1**, 379–383.
50 D. J. Darensbourg and A. I. Moncada, *Macromolecules*, 2010, **43**, 5996–6003.
51 X.-B. Lu and D. J. Darensbourg, *Chem. Soc. Rev.*, 2012, **41**, 1462–1484.
52 D. Tian, B. Liu, Q. Gan, H. Li and D. J. Darensbourg, *ACS Catal.*, 2012, **2**, 2029–2035.
53 Y. Yang, Y. Hayashi, Y. Fujii, T. Nagano, Y. Kita, T. Ohshima, J. Okuda and K. Mashima, *Catal. Sci. Technol.*, 2012, **2**, 509–513.
54 T. Ema, Y. Miyazaki, S. Koyama, Y. Yano and T. Sakai, *Chem. Commun.*, 2012, **48**, 4489.
55 B. Chatelet, L. Joucla, J.-P. Dutasta, A. Martinez, K. C. Szeto and V. Dufaud, *J. Am. Chem. Soc.*, 2013, **135**, 5348–5351.
56 M. A. Fuchs, T. A. Zevaco, E. Ember, O. Walter, I. Held, E. Dinjus and M. Döring, *Dalton Trans.*, 2013, **42**, 5322.
57 C. J. Whiteoak, N. Kielland, V. Laserna, F. Castro-Gómez, E. Martin, E. C. Escudero-Adán, C. Bo and A. W. Kleij, *Chem. – Eur. J.*, 2014, **20**, 2264–2275.
58 T. Werner and H. Büttner, *ChemSusChem*, 2014, **7**, 3268–3271.
59 S. Gennen, M. Alves, R. Méreau, T. Tassaing, B. Gilbert, C. Detrembleur, C. Jerome and B. Grignard, *ChemSusChem*, 2015, **8**, 1845–1849.
60 J. Rintjema and A. W. Kleij, *ChemSusChem*, 2017, **10**, 1274–1282.
61 S. Arayachukiat, C. Kongtes, A. Barthel, S. V. C. Vummaleti, A. Poater, S. Wannakao, L. Cavallo and V. D'Elia, *ACS Sustainable Chem. Eng.*, 2017, **5**, 6392–6397.
62 D. O. Meléndez, A. Lara-Sánchez, J. Martínez, X. Wu, A. Otero, J. A. Castro-Osma, M. North and R. S. Rojas, *ChemCatChem*, 2018, **10**, 2271–2277.
63 M. Hong, Y. Kim, H. Kim, H. J. Cho, M.-H. Baik and Y. Kim, *J. Org. Chem.*, 2018, **83**, 9370–9380.
64 Á. Mesías-Salazar, J. Martínez, R. S. Rojas, F. Carrillo-Hermosilla, A. Ramos, R. Fernández-Galán and A. Antiñolo, *Catal. Sci. Technol.*, 2019, **9**, 3879–3886.
65 H. Ma, J. Zeng, D. Tu, W. Mao, B. Zhao, K. Wang, Z. Liu and J. Lu, *Tetrahedron Lett.*, 2020, **61**, 151593.
66 W. Natongchai, J. A. Luque-Urrutia, C. Phungpanya, M. Solà, V. D'Elia, A. Poater and H. Zipse, *Org. Chem. Front.*, 2021, **8**, 613–627.
67 Q. Yao, Y. Shi, Y. Wang, X. Zhu, D. Yuan and Y. Yao, *Asian J. Org. Chem.*, 2022, **11**, e202200106.
68 S. Jana, H. Yu, A. Parthiban and C. L. L. Chai, *J. Polym. Sci., Part A: Polym. Chem.*, 2010, **48**, 1622–1632.
69 S. W. Hwang, D. H. Park, D. H. Kang, S. B. Lee and J. K. Shim, *J. Appl. Polym. Sci.*, 2016, **133**, 43388.
70 J. Sun, S. Fujita and M. Arai, *J. Organomet. Chem.*, 2005, **690**, 3490–3497.
71 M. Blain, L. Jean-Gérard, R. Auvergne, D. Benazet, S. Caillol and B. Andrioletti, *Green Chem.*, 2014, **16**, 4286–4291.
72 H.-Y. Ju, M.-D. Manju, K.-H. Kim, S.-W. Park and D.-W. Park, *J. Ind. Eng. Chem.*, 2008, **14**, 157–160.
73 L. Wang, G. Zhang, K. Kodama and T. Hirose, *Green Chem.*, 2016, **18**, 1229–1233.
74 X. Wang, L. Wang, Y. Zhao, K. Kodama and T. Hirose, *Tetrahedron*, 2017, **73**, 1190–1195.
75 C. J. Whiteoak, E. Martin, M. M. Belmonte, J. Benet-Buchholz and A. W. Kleij, *Adv. Synth. Catal.*, 2012, **354**, 469–476.
76 D. Gourgouillon, H. M. N. T. Avelino, J. M. N. A. Fareleira and M. Nunes da Ponte, *J. Supercrit. Fluids*, 1998, **13**, 177–185.
77 C. Kwag, C. W. Manke and E. Gulari, *J. Polym. Sci., Part B: Polym. Phys.*, 1999, **37**, 2771–2781.
78 *Footnote*: some experiments were conducted using a sapphire-windowed reactor and for pressures slightly above 100 bar (~120 bars), the entire mixture of toluene and CO_2 became supercritical, which triggered the precipitation of the Lotader® copolymers. This could explain the best compromise of 40–80 bar to achieve both good solubility and enhanced availability of CO_2 in the liquid toluene phase. See also: H. Zhang, Z. Liu and B. Han, *J. Supercrit. Fluids*, 2000, **18**, 185–192. We also tried the reaction in the absence of toluene (see Fig. S33, ESI†) and could not observe an efficient process and consistent conversions of epoxy-containing copolymers (see also Photo S1, ESI†).
79 B. Rainglet, P. Besognet, C. Benoit, K. Delage, V. Bounor-Legaré, C. Forest, P. Cassagnau and Y. Chalamet, *Polymers*, 2022, **14**, 4513.
80 L. Verny, N. Ylla, F. D. Cruz-Boisson, E. Espuche, R. Mercier, G. Sudre and V. Bounor-Legaré, *Ind. Eng. Chem. Res.*, 2020, **59**, 16191–16204.
81 C. Dubois, C. Marestin, P. Cassagnau, K. Delage, P. Alcouffe, N. Garois and V. Bounor-Legaré, *Polymer*, 2022, **254**, 125022.
82 R. R. A. Bolt, J. A. Leitch, A. C. Jones, W. I. Nicholson and D. L. Browne, *Chem. Soc. Rev.*, 2022, **51**, 4243–4260.
83 S. Martey, B. Addison, N. Wilson, B. Tan, J. Yu, J. R. Dorgan and M. J. Sobkowicz, *ChemSusChem*, 2021, **14**, 4280–4290.